


RESEARCH

Open Access



Screw placement through a higher medial portal provides better initial stability in arthroscopic ACL tibial avulsion fracture fixation: a finite element analysis

Yang Xiao¹, Changhao Shi¹, Geyang Deng¹, Zichu Ding¹, Jinhuan Xu² and Bin Chen^{1*} 

Abstract

Objective The objective of this study was to investigate the initial stability of different screw placements in arthroscopic anterior cruciate ligament (ACL) tibial avulsion fracture fixation.

Methods A three-dimensional knee model at 90° flexion was utilized to simulate type III ACL tibial avulsion fracture and arthroscopic screw fixation through different portals, namely the central transpatellar tendon portal (CTP), anterolateral portal (ALP), anteromedial portal (AMP), lateral parapatellar portal (LPP), medial parapatellar portal (MPP), lateral suprapatellar portal (LSP), medial suprapatellar portal (MSP). A shear force of 450 N was applied to the finite element models at 30° flexion to simulate the failure condition. The displacement of the bony fragment and the volume of the bone above 25,000 μ -strain (damaged bone volume) were calculated around the screw path.

Results When the screw was implanted through CTP, the displacement of the bony fragment reached the maximum displacement which was 1.10 mm and the maximum damaged bone volume around the screw path was 148.70 mm³. On the other hand, the minimum displacement of the bony fragment was 0.45 mm when the screw was implanted through LSP and MSP. The minimum damaged bone volume was 14.54 mm³ around the screw path when the screw was implanted through MSP.

Conclusion Screws implanted through a higher medial portal generated less displacement of the bony fragment and a minimum detrimental strain around the screw path. The findings are clinically relevant as they provide biomechanical evidence on optimizing screw placement in arthroscopic ACL tibial avulsion fracture fixation.

Keywords ACL avulsion fracture, Arthroscopic screw fixation, Portal, Biomechanical effect, Finite element analysis

*Correspondence:

Bin Chen

chenbin1@smu.edu.cn

¹Division of Orthopaedics and Traumatology, Department of Orthopaedics, Nanfang Hospital, Southern Medical University, Guangzhou, China

²Department of Trauma and Joint Surgery, The Fourth Hospital affiliated to the Guangzhou Medical University, Guangzhou, China



© The Author(s) 2024. **Open Access** This article is licensed under a Creative Commons Attribution 4.0 International License, which permits use, sharing, adaptation, distribution and reproduction in any medium or format, as long as you give appropriate credit to the original author(s) and the source, provide a link to the Creative Commons licence, and indicate if changes were made. The images or other third party material in this article are included in the article's Creative Commons licence, unless indicated otherwise in a credit line to the material. If material is not included in the article's Creative Commons licence and your intended use is not permitted by statutory regulation or exceeds the permitted use, you will need to obtain permission directly from the copyright holder. To view a copy of this licence, visit <http://creativecommons.org/licenses/by/4.0/>. The Creative Commons Public Domain Dedication waiver (<http://creativecommons.org/publicdomain/zero/1.0/>) applies to the data made available in this article, unless otherwise stated in a credit line to the data.

Introduction

Anterior cruciate ligament (ACL) tibial avulsion fractures are relatively rare injuries that occur mostly in children and adolescents aged 8–14 [1]. These injuries can also occur in adults and are equivalent to acute ACL ruptures [2]. Avulsion fractures commonly involve the intercondylar depression, where the ACL insertion lies. The fracture has been classified into three types (type I, II and III) according to the severity of displacement by Meyers and McKeever [3]. Zaricznyj applied this classification with a type IV for comminuted fractures [4]. Conservative treatment results are ineffective for type III fractures, so surgical operation should be considered [5, 6]. Arthroscopic reduction and fixation with screws or sutures are the mainstream treatment for these fractures unless other lesions require open surgery [2].

Assessment of the clinical outcome of screw and suture fixation remains ambiguous. According to the latest systematic review and meta-analysis, there are no significant differences in clinical outcome scores between the two approaches [7]. Screw fixation is relatively simple and allows the surgeon to maintain compression of the fracture fragments, whereas the suture fixation has a decreased risk of implant removal [8]. A single 3.5–4.0 mm screw is sufficient to maintain the bony fragment in place in the case of arthroscopic screw fixation [9–11]. Screws are usually implanted at a high knee flexion angle [10, 11]. The objective of ACL avulsion fracture treatment is to restore the isometry and tension of the ACL by anatomic reduction and fixation. Malunion and prolonged knee instability may be caused by the potential displacement of the bony fragment, even requiring revision surgery [9, 12–14]. Therefore, studying the initial stability of the fixed ACL complex after surgery is necessary. The screw has been reported in previous clinical or biomechanical studies to be implanted through a particular portal or the dissected knee joint [9–11, 15–17]. The influence of screw placement through different portals on the biomechanical behaviour of the fixed ACL complex is little understood. However, different portals will change the orientation of the screw in the bone, which may affect the stability of the bony fragment under the tension of the ACL. Understanding the biomechanical differences caused by the surgical portal could provide the foundation for optimizing surgery. This study aims to investigate the initial stability of different screw placements in arthroscopic ACL tibial avulsion fracture fixation.

Finite element models were developed to simulate the failure condition and evaluate the displacement of the bony fragment and the strain around the screw path in this study. The strain above 25,000 μ -strain

was considered as fracture strength of the bone [18]. To the knowledge of the authors, this is the first study to explore the biomechanical stability of screw placement orientation in ACL tibial avulsion fracture fixation. The hypothesis was that screw insertion through a higher medial portal would offer better initial stability, resulting in less displacement of the bony fragment and a minimum detrimental strain surrounding the screw path.

Materials and methods

Establishment of the three-dimensional (3D) models

The 3D models from the previous work of the authors were employed in the present study as well [19]. The right knee of a healthy volunteer was imaged using computed tomography (CT) (SOMATOM Definition AS+; Siemens) with a thickness of 0.6 mm and resolution of 512×512 pixels. The 3D models of the femur and tibia were reconstructed from the CT images in Mimics (v19.0, Materialize NV, Leuven, BE). The knee models at 30° and 90° flexion were obtained by matching their outlines to the corresponding fluoroscopic images during a lunging motion.

Surgical modelling

Seven distinct arthroscopic portals around the patella were identified on the knee model at 90° flexion (Fig. 1a). The central transpatellar tendon portal (CTP) was discovered in the centre of the patellar tendon just under the inferior edge of the patella. The anterolateral portal (ALP) and anteromedial portal (AMP) were aligned with the inferior edge of the patella on both sides of the patellar tendon. The lateral parapatellar portal (LPP) and medial parapatellar portal (MPP) were located 5 mm from the lateral and medial edge of the patella. The lateral suprapatellar portal (LSP) and medial suprapatellar portal (MSP) were identified at the junction of the tangential line between the superior and medial/lateral edges of the patella.

The tibial and femoral footprint of the ACL were determined by the bony landmarks as described in the previous article [19]. The bony fragment was located on the position of ACL tibial insertion. A hemispherical bony fragment with a diameter of 12 mm was designed to ensure the orientation of the screw as the sole variable. All insertion points of the screws were the same, located in the centre of the bony fragment. According to a previous study, a screw should not be larger than one-third of the diameter of the bone fragment to prevent comminution [20]. Therefore, each screw was designed with a diameter of 3.5 mm and a length of 28 mm. The orientation of the screw was dictated by the position of the portal and the insertion point of the screw. Figure 1b shows the various screws

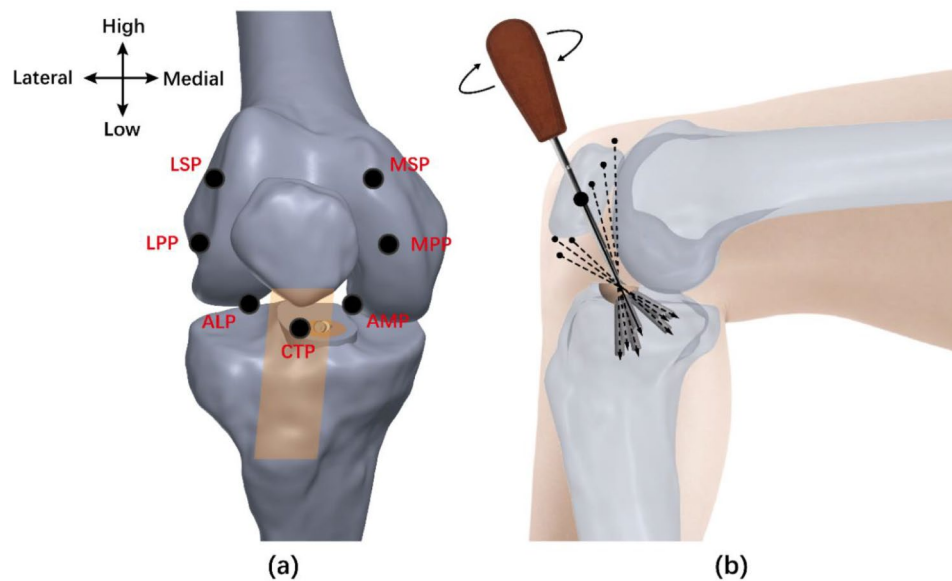


Fig. 1 (a) Identification of the arthroscopic portals of the knee joint (CTP central transpatellar tendon portal; ALP anterolateral portal; AMP anteromedial portal; LPP lateral parapatellar portal; MPP medial parapatellar portal; LSP lateral suprapatellar portal; MSP medial suprapatellar portal; orange parallelogram patellar tendon). (b) The various screws were implanted through different portals

through different portals. All modelling procedures were performed using SolidWorks (v2018, Dassault Systemes, Massachusetts, USA).

Finite element models of the knee joint

The 3D models were exported into the finite element analysis software Abaqus (v2018; Dassault Systèmes SE, Vélizy-Villacoublay, FR). The femur was assumed a shell and defined as a rigid body. The bony fragment and tibia were assumed solids and were defined as a homogeneous isotropic elastic material with Young's modulus $E=389$ MPa and Poisson's ratio $\nu=0.3$ [21]. The material of the screw was stainless steel and was defined as a homogeneous isotropic material with Young's modulus $E=205$ GPa and Poisson's ratio $\nu=0.3$ [22]. The ACL was assumed to be solid and was defined as a homogeneous isotropic elastic material with Young's modulus $E=345$ MPa and Poisson's ratio $\nu=0.45$ [23]. A free meshing technique was applied for the entire model (femur: four-node 3-D bilinear rigid quadrilateral element, element type: R3D4; bony fragment and tibia: four-node linear tetrahedron element, element type: C3D4; screw and ACL: eight-node linear hexahedral element, element type: C3D8).

Bonded contact between the ACL and the femur and between the ACL and the top face of the bony fragment were defined. For both models, the screw-bone contact interfaces and the bony fragment-tibia contact interfaces were modelled as sliding interactions with a friction coefficient of 0.3 [24]. The screw tightening preload of 300 N was used to tighten the screw. The compression effect of the screw on the bony fragment was accurately simulated

by defining a bonded contact between the screw head and the top face of the bony fragment. The mid-lower part of the tibia was fixed. Studies have reported that the fixed ACL complex was loaded in the range of 30–450 N for the rehabilitation process, depending on the activity [25–27]. A posterior shear force of 450 N was applied to the femur at 30° of knee flexion to simulate an anterior tibial displacement (Fig. 2a). The displacement of the bony fragment and the strain around the screw path were subsequently calculated. The volume of strain above 25,000 μ -strain on the bone was recorded (Fig. 2b, c).

Validation of finite element models

A finite element model of arthroscopic screw fixation through AMP was first established and analysed. To perform mesh sensitivity analysis, stepwise upsizing on the mesh size was applied [28]. The convergence tolerance was set as a variation of stress within 5% from the previous model with higher mesh density. The finally used mesh size of the screw, the bony fragment and the ACL were 0.5 mm, 0.5 mm and 1.0 mm, respectively. The mesh size of the tibia was 1.5 mm, and mesh refinement was performed on the 0.5 mm contact with the bony fragment and screw (Table 1). The initial displacement of the bony fragment was compared to the literature results [15–17] (Table 2).

To validate the results obtained through finite element analysis, a tensile testing simulation was performed according to the previous mechanical study [29]. The tibia-ACL-femur model was applied to a tensile load along the axis of the ACL at 30° of knee flexion (Fig. 3). The tensile load was beginning at 450 N

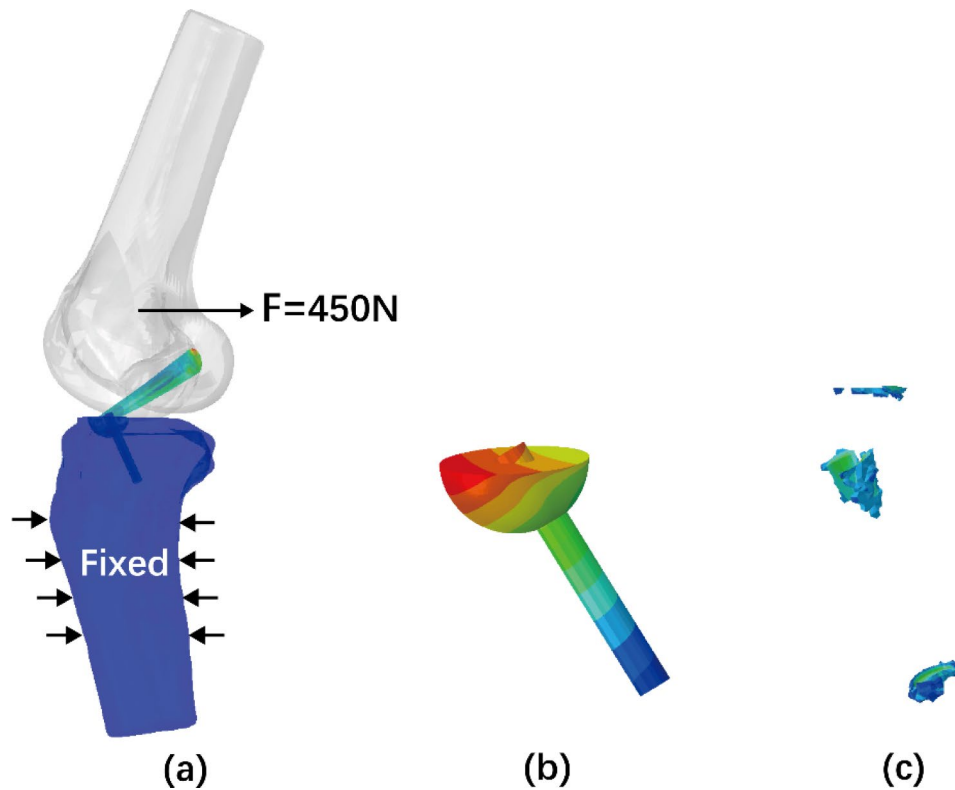


Fig. 2 (a) The mid-lower part of the tibia was fixed and a posterior shear force was applied at the femur at 30° of knee flexion; (b) The maximum displacement of the fixed bony fragment was calculated. (c) The volume of strain on the bone above 25,000 μ -strain was recorded

Table 1 Numbers of nodes and elements of the four components

Components	Nodes	Elements
Screw	4,389	3,640
Bony fragment	7,431	37,172
ACL	3,367	2,772
Tibia	70,118	379,772

Table 2 Comparisons of initial displacement of the bony fragment in the present study and previous studies

Study	Applied maximum load to failure (N)	Initial displacement (mm)
Present study	450	0.88
Ezechieli et al. [16]	311.7 \pm 120.3	0.84 \pm 0.15
Eggers et al. [15]	457.1 \pm 13.4	2.17 \pm 1.4
In et al. [17]	101.8 \pm 29.0	0.4 \pm 0.2

and incrementally increased by 20 N up to 530 N. The load-elongation curve was constructed, and the angular coefficient of the linear equation was compared to the experimental result (Fig. 4). The results of comparison showed that a variance of 4.92% exists between the finite element analysis and mechanical test within the discrepancy threshold of 20% [30]. Therefore, the finite element model can be used in subsequent

research, as it exhibits similar structural properties to mechanical testing.

Results

In both medial (MLP, MPP and MSP) and lateral portals (ALP, LPP and LSP), the displacement of the bony fragment gradually decreased when portals were located higher. The maximum displacement of the bony fragment was 1.10 mm when the screw was implanted through CTP. On the other hand, the minimum displacement of the bony fragment was 0.45 mm when the screw was implanted through LSP and MSP. The average displacement of the bony fragment was 0.68 mm and 0.65 mm, for the lateral and medial portals, respectively (Fig. 5a).

In both medial and lateral portals, the damaged bone volume decreased when portals were located higher. The maximum volume of strain above 25,000 μ -strain on the bone was 148.70 mm³ when the screw was implanted through CTP. Correspondingly, the minimum volume of strain above 25,000 μ -strain on the bone was 14.54 mm³ when the screw was implanted through MSP. For the lateral and medial portals, the average volume of the damaged bone was 56.95 mm³ and 44.96 mm³, respectively (Fig. 5b). The distribution of the damaged bone for each model is shown in Fig. 6.

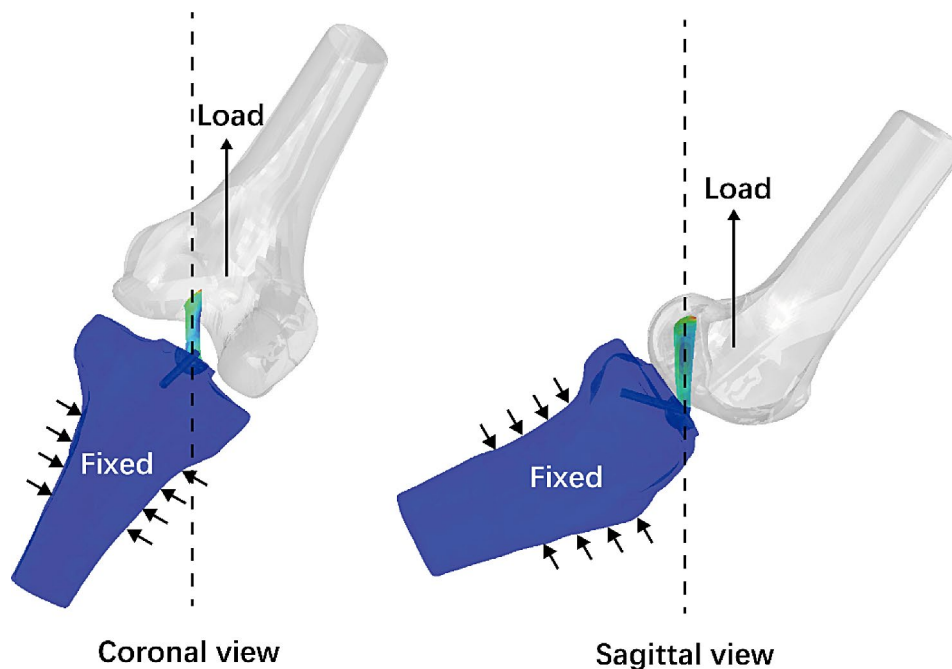


Fig. 3 Schematic of tensile testing. The tensile load was applied along the axis of the ACL while the normal anatomical angles of ACL were preserved

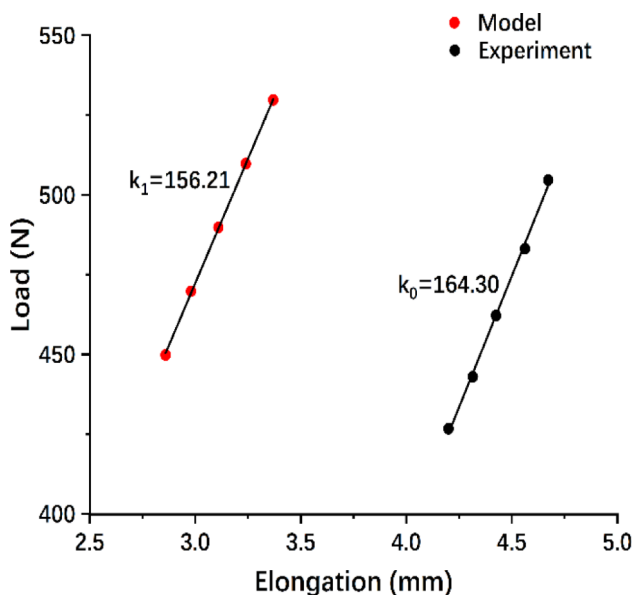


Fig. 4 Load-elongation curves for tensile testing demonstrate the similarities in results between the model and experiment

Figure 7 showed the stress distribution on the bone for each model. Various stress distribution patterns existed due to the different screw insertions. The stress concentration point on the bony fragment occurred at the posterior contact surface between the two bones in all models. The stress concentration point on the tibia occurred at the end of the screw in LPP and LSP models, occurred at the posterior contact surface between the two bones in MPP and MSP models, and occurred at the junction

between the two bones and screw in CTP, ALP and AMP models. The maximum Mises stresses were 33.00 MPa and 44.07 MPa on the bony fragment and the tibia, respectively, when the screw was implanted through CTP. The minimum Mises stresses were 16.25 MPa and 22.97 MPa on the bony fragment and the tibia, respectively, when the screw was implanted through LSP and MSP.

Discussion

The most noteworthy finding of the present study was that screws implanted from different portals could impact the displacement of the bony fragment and the strain on the bone around the screw path. Screws that were implanted through a higher medial portal resulted in less displacement of the bony fragment and a minimum damaging strain around the screw path. The current findings are of clinical relevance as they might provide biomechanical evidence to optimize screw placement in arthroscopic ACL tibial avulsion fracture fixation.

The initial stability is essential to the risk of residual laxity and could predict potential loss in reduction during healing after surgery [31]. Previous research on biomechanics has focused on comparing the strength of screw fixation and suture techniques [15, 31–34]. Sometimes studies favour either screws or sutures, while other times reporting no significant difference between them. Eggers et al. [15] reported that a second screw has no positive effect on the biomechanical characteristics than one-screw fixation. Regarding the method of screw placement, Ezechieli et al. [16] and In et al. [17] used

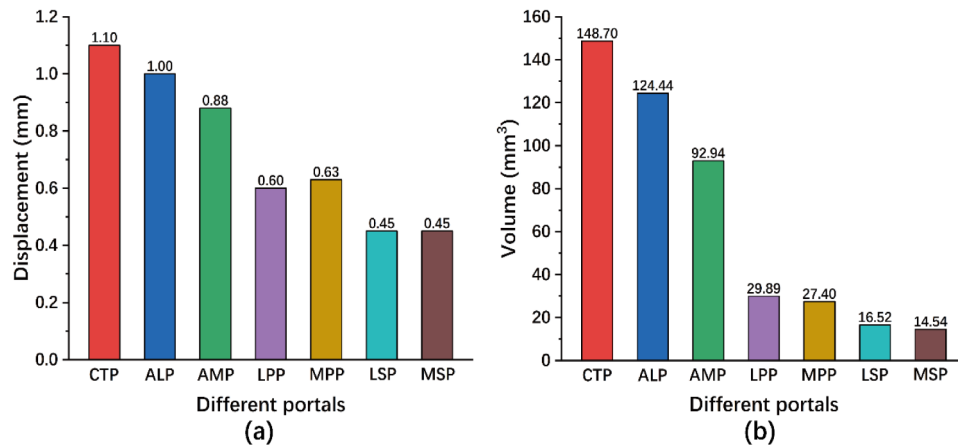


Fig. 5 Comparison of (a) the maximum displacement of the bony fragment and (b) the volume of strain on the bone above 25,000 μ -strain among the different portals

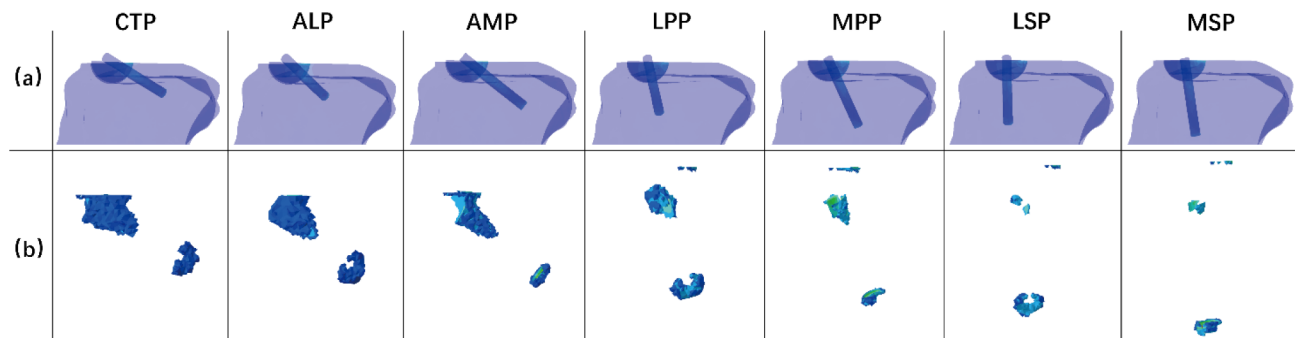


Fig. 6 The distribution of the damaged bone for each model. (a) The position of the screw in the bone from the sagittal view; (b) The damaged bone around the screw path

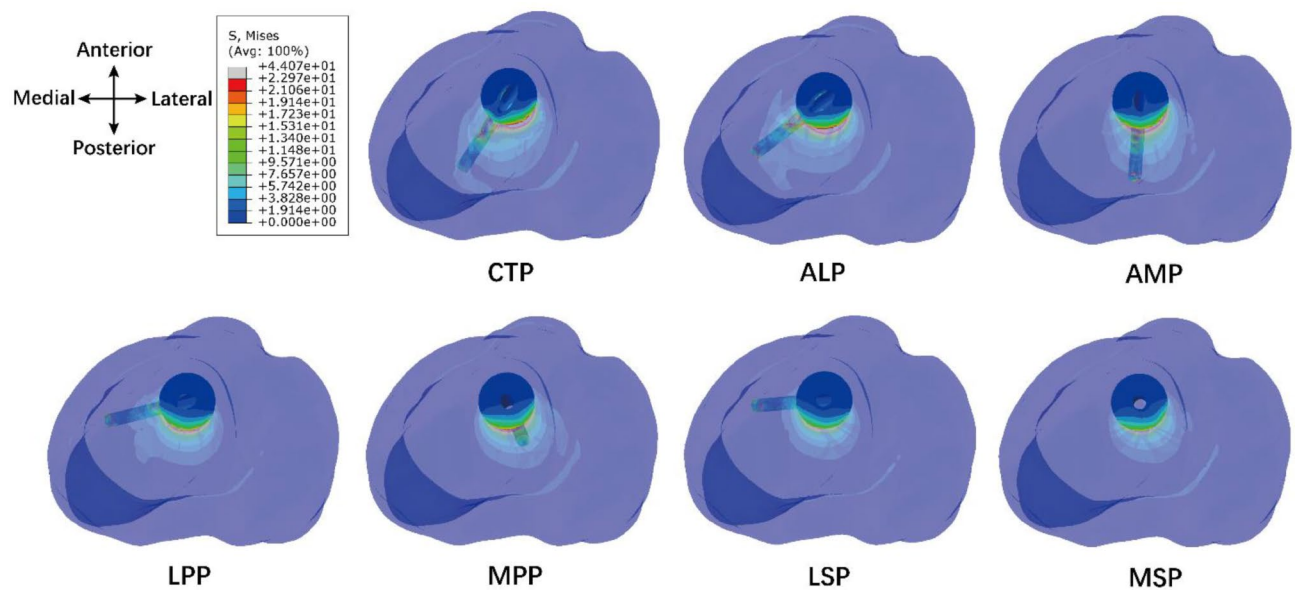


Fig. 7 Distribution of Mises stress on bony fragment and tibia through a view perpendicular to the tibial plateau

the dissected knee joint to implant the screw, which was inconsistent with the condition of arthroscopic screw fixation. As for the arthroscopic portal for screw implanting, Hunter et al. [9] implanted the screw through CTP and Lubowitz et al. [10] through AMP. Senekovic et al. [11] implanted the screw through a superior antero-medial portal, higher than AMP and lower than MPP. However, there is no consensus on the effect of different portals on the biomechanical stability of the screw. To the knowledge of the authors, this is the only study to explore the biomechanical stability of screw placement orientation in ACL tibial avulsion fractures. The results showed that CTP might not be a good choice when implanting the screw with the arthroscopic technique. Instead, it might be better to implant the screw through a higher medial portal as much as possible.

Experiments in previous biomechanical studies were performed at specific knee flexion angles, approximately in the Lachmann position [15, 34]. Cyclical loading forces such as anterior shear or upward traction force were applied to the tibia or femur to simulate the failure conditions [15, 17]. In the current study, shear loads were applied at 30° of knee flexion to be consistent with in vitro experiments. Standardized cubic bony fragments with various sizes have usually been created in previous studies to simulate the ACL tibial avulsion fracture [17, 32]. Considering the experimental rigour, hemispherical bony fragments were hereby used to ensure that the screw orientation was the only variable, although it was inconsistent with the clinical fracture pattern. In addition, simplification of tissue properties was performed in this study, which would affect the magnitude but not the tendency of calculated results. Even so, validation results showed that the structural properties and elastic deformations of the model were reliable.

The pull-out of the screw and fracture of the fragment were two main failure modes in previous literature, with the former one being the most common. Ezechieli et al. [16] reported 60% screw pull-out failure and 40% fragment fracture failure. In et al. [17] reported 86% screw pull-out failure and 14% fragment fracture failure. Bong et al. [32] found the single observed failure mode for the specimens was screw pull-out from the cancellous bone of the fracture bed. Unlike other failure modes of fracture internal fixation, none of the literature studies has reported screw breakage in treating ACL tibial avulsion fractures. Feng et al. [35] indicated that screw loosening is closely related to bone damage caused by abnormal stress around the screw. That was the reason why this study investigated the damaged bone volume around the screw path. The damaged bone was mainly concentrated at the junction of the bony fragment and the tibia and the end of the screw, which could reduce the stability of the

screw (Fig. 6). The smaller the damaged bone volume, the less probability the screw would pull out from the bone.

This study has several limitations. First, only one direction of force was applied, and the cyclical loading force from daily knee motion, such as walking, was not analyzed. In fact, the force of the ACL is quite complex, depending on different activities. Additionally, the bony fragment is idealized as a hemisphere, which is inconsistent with the actual situation. The simplification to be able to control the single variable is necessary. The thread of the screw was not considered, and only one size of the screw was explored in this study, which is not entirely consistent with clinical practice. However, different screw sizes may affect the biomechanical effect of screw fixation. Since this study was mainly designed to explore the impact of different surgical portals on the initial stability of screw fixation, these factors may not affect the conclusions. Furthermore, the current study did not take into account the growth plate presence, which might challenge the surgeon's decision to select the portal when treating children and adolescents.

Conclusion

The findings of this study demonstrate that screw insertion through a higher medial portal improves the initial stability in arthroscopic ACL tibial avulsion fracture fixation, resulting in less displacement of the bony fragment and a minimum detrimental strain surrounding the screw path. Although there is no clear advantage of screw fixation compared with suture fixation in the treatment of ACL tibial avulsion fracture. The results are clinically relevant as they provide biomechanical evidence on optimizing screw placement in arthroscopic ACL tibial avulsion fracture fixation.

Abbreviations

ACL	Anterior Cruciate Ligament
CTP	Central Transpatellar tendon Portal
ALP	Anterolateral Portal
AMP	Anteromedial Portal
LPP	Lateral Parapatellar Portal
MPP	Medial Parapatellar Portal
LSP	Lateral Suprapatellar Portal
MSP	Medial Suprapatellar Portal
3D	Three-Dimensional
CT	Computed Tomography

Acknowledgements

Not applicable.

Author contributions

Y.X. designed and drafted the manuscript. C.S. and G.D. acquired the data. Z.D. and J.X. analyzed and interpreted the data. B.C. revised the manuscript. All authors read and approved the final version of the manuscript.

Funding

This work was sponsored by the National Natural Science Foundation of China (Grant No.12272164) and the Science and Technology Program of Guangzhou, China (Grant No.202102080570).

Data availability

The data that support the findings of this study are available from the corresponding author upon reasonable request.

Declarations

Ethical approval and consent to participate

This study was approved by the Institutional Review Board of Shanghai Jiao Tong University (ChiCTR-RPC-17013341). Written informed consent were obtained from the subject involved in the study. The study was performed following the Declaration of Helsinki principles.

Consent for publication

Not applicable.

Competing interests

The authors declare no competing interests.

Received: 13 December 2023 / Accepted: 16 July 2024

Published online: 20 July 2024

References

- Skak SV, Jensen TT, Poulsen TD, Stürup J. Epidemiology of knee injuries in children. *Acta Orthop Scand*. 1987;58(1):78–81.
- Bogunovic L, Tarabichi M, Harris D, Wright R. Treatment of tibial eminence fractures: a systematic review. *J Knee Surg*. 2015;28(3):255–62.
- Meyers MH, McKeever FM. Fracture of the intercondylar eminence of the tibia. *J Bone Joint Surg Am*. 1970;52(8):1677–84.
- Zaricznyj B. Avulsion fracture of the tibial eminence: treatment by open reduction and pinning. *J Bone Joint Surg Am*. 1977;59(8):1111–4.
- Lowe J, Chaimsky G, Freedman A, Zion I, Howard C. The anatomy of tibial eminence fractures: arthroscopic observations following failed closed reduction. *J Bone Joint Surg Am*. 2002;84(11):1933–8.
- Tudisco C, Giovannuscio R, Febo A, Savarese E, Bisicchia S. Intercondylar eminence avulsion fracture in children: long-term follow-up of 14 cases at the end of skeletal growth. *J Pediatr Orthop B*. 2010;19(5):403–8.
- Chang CJ, Huang TC, Hoshino Y, Wang CH, Kuan FC, Su WR, Hong CK. Functional outcomes and subsequent Surgical procedures after arthroscopic suture Versus Screw fixation for ACL tibial avulsion fractures: a systematic review and Meta-analysis. *Orthop J Sports Med*. 2022;10(4):23259671221085945.
- Shin YW, Uppstrom TJ, Haskel JD, Green DW. The tibial eminence fracture in skeletally immature patients. *Curr Opin Pediatr*. 2015;27(1):50–7.
- Hunter RE, Willis JA. Arthroscopic fixation of avulsion fractures of the tibial eminence: technique and outcome. *Arthroscopy*. 2004;20(2):113–21.
- Lubowitz JH, Grauer JD. Arthroscopic treatment of anterior cruciate ligament avulsion. *Clin Orthop Relat Res*. 1993;294:242–6.
- Senekovic V, Veselko M. Anterograde arthroscopic fixation of avulsion fractures of the tibial eminence with a cannulated screw: five-year results. *Arthroscopy*. 2003;19(1):54–61.
- Kocher MS, Foreman ES, Micheli LJ. Laxity and functional outcome after arthroscopic reduction and internal fixation of displaced tibial spine fractures in children. *Arthroscopy*. 2003;19(10):1085–90.
- Mah JY, Adili A, Otsuka NY, Ogilvie R. Follow-up study of arthroscopic reduction and fixation of type III tibial-eminence fractures. *J Pediatr Orthop*. 1998;18(4):475–7.
- Mulhall KJ, Dowdall J, Grannell M, McCabe JP. Tibial spine fractures: an analysis of outcome in surgically treated type III injuries. *Injury*. 1999;30(4):289–92.
- Eggers AK, Becker C, Weimann A, Herbort M, Zantop T, Raschke MJ, Petersen W. Biomechanical evaluation of different fixation methods for tibial eminence fractures. *Am J Sports Med*. 2007;35(3):404–10.
- Ezechieli M, Schäfer M, Becher C, Dratzidis A, Glaab R, Ryf C, Hurschler C, Ettinger M. Biomechanical comparison of different fixation techniques for reconstruction of tibial avulsion fractures of the anterior cruciate ligament. *Int Orthop*. 2013;37(5):919–23.
- In Y, Kwak DS, Moon CW, Han SH, Choi NY. Biomechanical comparison of three techniques for fixation of tibial avulsion fractures of the anterior cruciate ligament. *Knee Surg Sports Traumatol Arthrosc*. 2012;20(8):1470–8.
- Frost HM. A 2003 update of bone physiology and Wolff's Law for clinicians. *Angle Orthod*. 2004;74(1):3–15.
- Xiao Y, Ling M, Liang Z, Ding J, Zhan S, Hu H, Chen B. Dual fluoroscopic imaging and CT-based finite element modelling to estimate forces and stresses of grafts in anatomical single-bundle ACL reconstruction with different femoral tunnels. *Int J Comput Assist Radiol Surg*. 2021;16(3):495–504.
- Berg EE. Pediatric tibial eminence fractures: arthroscopic cannulated screw fixation. *Arthroscopy*. 1995;11(3):328–31.
- El'Sheikh HF, MacDonald BJ, Hashmi MSJ. Finite element simulation of the hip joint during stumbling: a comparison between static and dynamic loading. *J Mater Process Technol*. 2003;143–144:249–55.
- Benli S, Aksoy S, Havitcioğlu H, Kucuk M. Evaluation of bone plate with low-stiffness material in terms of stress distribution. *J Biomech*. 2008;41(15):3229–35.
- Uğur L. Comparison of reaction forces on the anterior cruciate and anterolateral ligaments during internal rotation and anterior drawer forces at different flexion angles of the knee joint. *Int J Med Robot*. 2017;13:e1815.
- MacLeod AR, Pankaj P, Simpson AH. Does screw-bone interface modelling matter in finite element analyses? *J Biomech*. 2012;45(9):1712–6.
- Beynonn BD, Amis AA. In vitro testing protocols for the cruciate ligaments and ligament reconstructions. *Knee Surg Sports Traumatol Arthrosc*. 1998;6(1):570–76.
- Holden JP, Grood ES, Korvick DL, Cummings JF, Butler DL, Bylski-Austrow DI. In vivo forces in the anterior cruciate ligament: direct measurements during walking and trotting in a quadruped. *J Biomech*. 1994;27(5):517–26.
- Morrison JB. The mechanics of the knee joint in relation to normal walking. *J Biomech*. 1970;3(1):51–61.
- Orsi AD, Chakravarthy S, Canavan PK, Peña E, Goebel R, Vaziri A, Nayeb-Hashemi H. The effects of knee joint kinematics on anterior cruciate ligament injury and articular cartilage damage. *Comput Methods Biomech Biomed Engin*. 2016;19(5):493–506.
- Woo SL, Hollis JM, Adams DJ, Lyon RM, Takai S. Tensile properties of the human femur-anterior cruciate ligament-tibia complex. The effects of specimen age and orientation. *Am J Sports Med*. 1991;19(3):217–25.
- Hsu CC, Chao CK, Wang JL, Hou SM, Tsai YT, Lin J. Increase of pullout strength of spinal pedicle screws with conical core: biomechanical tests and finite element analyses. *J Orthop Res*. 2005;23(4):788–94.
- Mahar AT, Duncan D, Oka R, Lowry A, Gillingham B, Chambers H. Biomechanical comparison of four different fixation techniques for pediatric tibial eminence avulsion fractures. *J Pediatr Orthop*. 2008;28(2):159–62.
- Bong MR, Romero A, Kubiak E, Lesaka K, Heywood CS, Kummer F, Rosen J, Jazrawi L. Suture versus screw fixation of displaced tibial eminence fractures: a biomechanical comparison. *Arthroscopy*. 2005;21(10):1172–6.
- Hapa O, Barber FA, Süner G, Özden R, Davul S, Bozdağ E, Sünbüloğlu E. Biomechanical comparison of tibial eminence fracture fixation with high-strength suture, EndoButton, and suture anchor. *Arthroscopy*. 2012;28(5):681–7.
- Tsukada H, Ishibashi Y, Tsuda E, Hiraga Y, Toh S. A biomechanical comparison of repair techniques for anterior cruciate ligament tibial avulsion fracture under cyclic loading. *Arthroscopy*. 2005;21(10):1197–201.
- Feng X, Lin G, Fang CX, Lu WW, Chen B, Leung FKL. Bone resorption triggered by high radial stress: the mechanism of screw loosening in plate fixation of long bone fractures. *J Orthop Res*. 2019;37(7):1498–507.

Publisher's Note

Springer Nature remains neutral with regard to jurisdictional claims in published maps and institutional affiliations.